Magnetite Nanoparticles are Metastable Biogeobatteries in Consecutive Redox Cycles Driven by Microbial Fe Oxidation and Reduction

T. Bayer[1], N. Jakus[1, †], A. Kappler[1,2] and J.M. Byrne[3, *]

[1]Geomicrobiology Group, Department of Geosciences, University of Tuebingen, Schnarrenbergstrasse 94-96, 72076 Tuebingen, Germany

[†]Current address: Environmental Microbiology Laboratory, École Polytechnique Fédérale de Lausanne, CE1 644, Lausanne CH 1015, Switzerland.

[2]Cluster of Excellence: EXC 2124: Controlling Microbes to Fight Infection, Tuebingen, Germany.

[3]School of Earth Sciences, University of Bristol, Queens Road BS8 1RJ, Bristol, United Kingdom

SUPPLEMENTARY MATERIAL

Number of figures: 6

Number of tables: 2

Total number of pages: 10

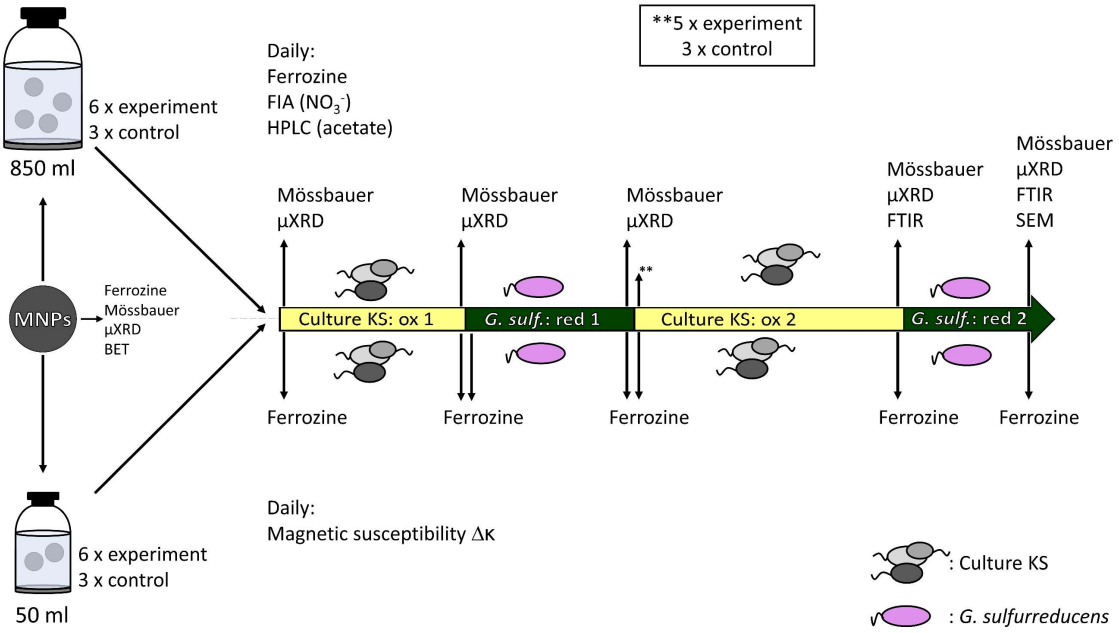

Figure S1. Overview of samplings performed before and during the experiment with magnetite nanoparticles as biogeobatteries in two consecutive redox cycles with the nitrate-reducing Fe(II)-oxidizing culture KS and the Fe(III)-reducer *G. sulfurreducens* over 41 days.

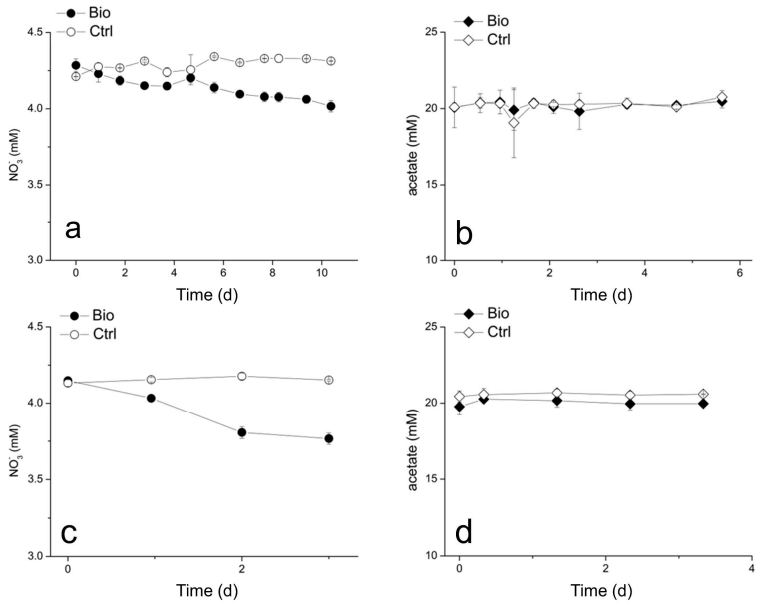

Figure S2. (a+c) Measured changes of nitrate during first and second oxidation, respectively, (b+d) measured acetate during first and second reduction. Not all time points were sampled as Fe(II)/Fe(III) samples were preferentially treated. Panels a and c: As expected, NO_3^- decreased during growth of culture KS (a+c). Panels b and d: Since acetate was supplied in excess, no changes could be determined via HPLC Please note that the y-axis starts at 3.0 mM for nitrate and 10 mM for acetate.

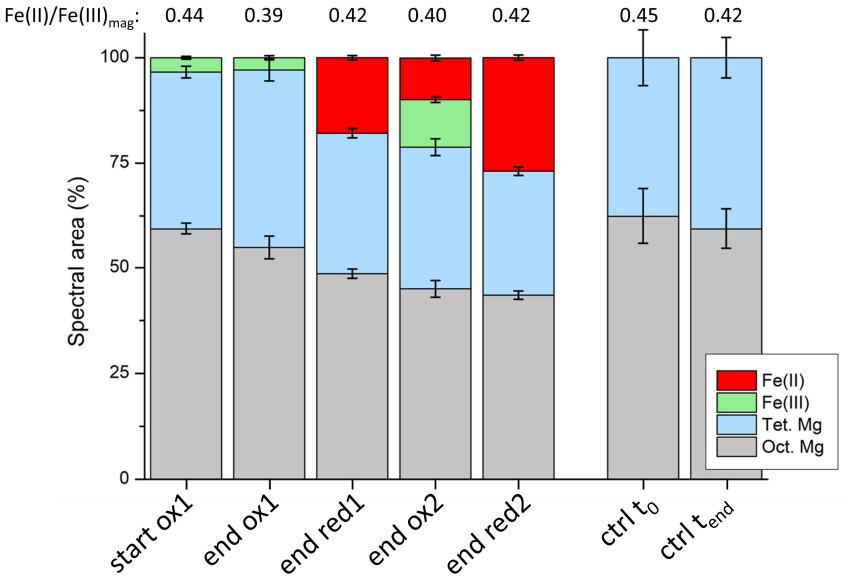

Figure S3. Relative abundances of spectral areas collected with ^{57}Fe Mössbauer spectroscopy. Displayed are octahedral magnetite (Oct. Mg, grey), tetrahedral magnetite (Tet. Mg, light blue), Fe(III) (light green) and Fe(II) (red). The numbers above stacked columns display the determined Fe(II)/Fe(III) ratio of magnetite in the respective sample ($Fe(II)/Fe(III)_{mag}$).

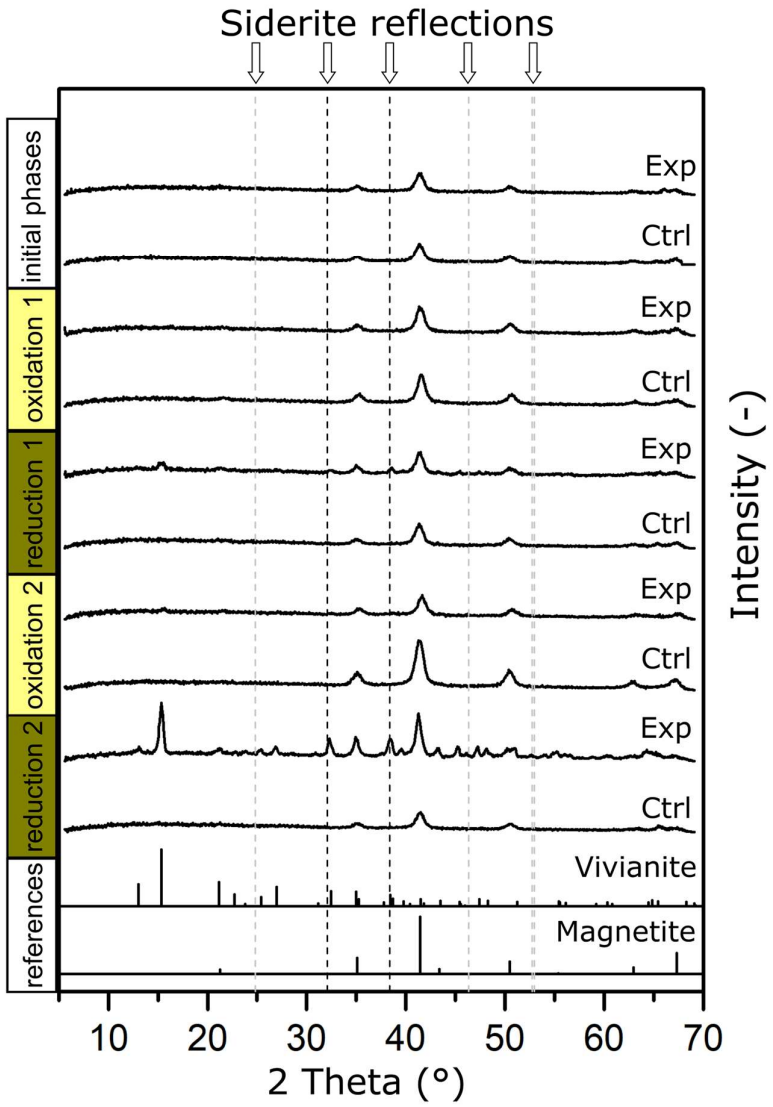

Figure S4. µXRD samples displayed with 6 major reflections of siderite (2θ of 24.85°, 32.12°, 38.45°, 46.33°, 52.92°, 53.1°). Two black dotted lines overlap with samples (32.12°, 38.45°), especially after the second reduction. Additional lines (grey) show major reflections of siderite that were not detected in our samples.

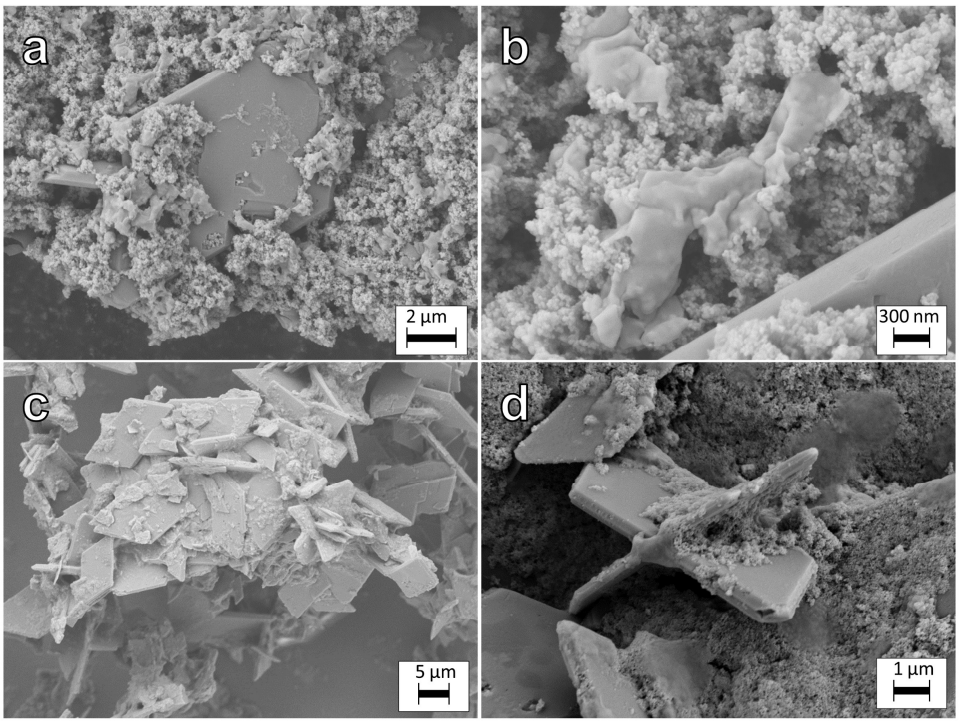

Figure S5. SEM images from samples taken after the final reduction. (a) vivianite with surface/crystal defects and in close contact with MNPs (b) remains of microbial biomass/cells. (c) Conglomerate of vivianite crystals (d) vivianite crystals with characteristic twinning and in close contact with MNPs.

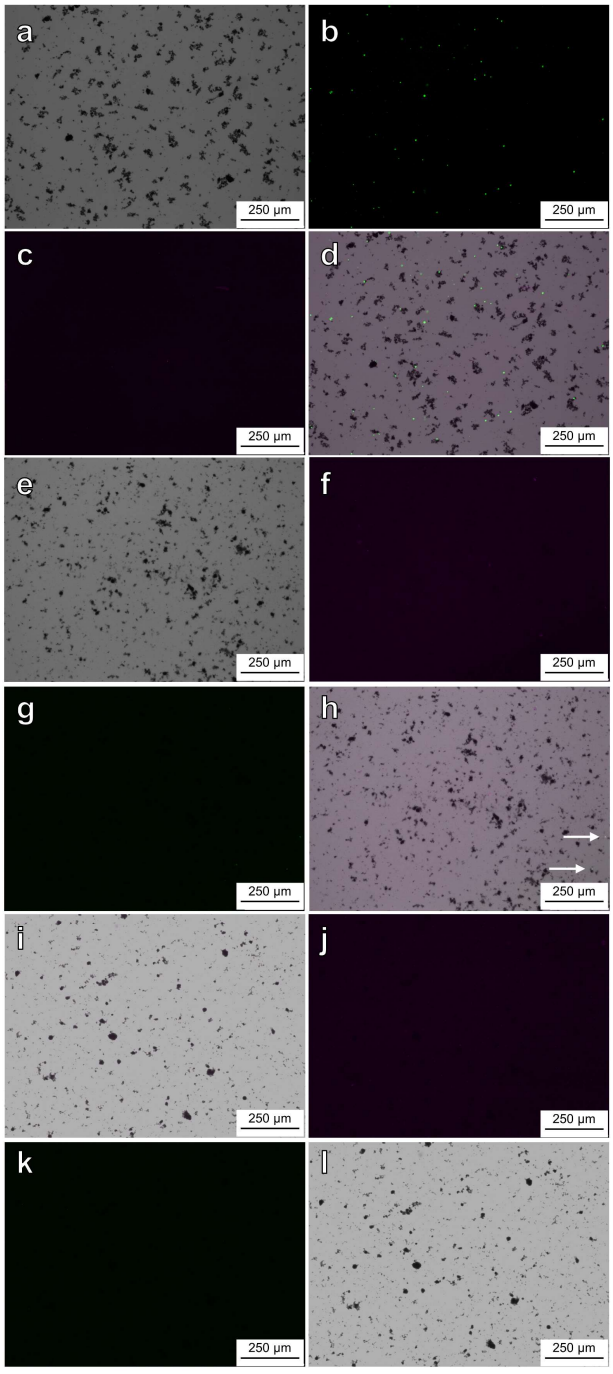

Figure S6. Light/fluorescence microscopy images of culture KS before and after washing steps. (a-d) brightfield, live, dead and overlayed channels of culture KS that was not yet washed. (e-h) brightfield, live, dead and overlayed channels of culture KS that was washed 3 times. Notice that still some cells could be seen (white arrows) (i-l) brightfield, live, dead, and overlayed channels of culture KS that was washed 5 times, no more cells could be detected.

Table S1. Properties of MNPs during incubation with culture KS and *G. sulfurreducens*. Crystal size, lattice parameter and Fe(II)/Fe(III) ratio determined by µXRD. Fe(II)/Fe(III) ratio determined by the spectrophotometric ferrozine assay and Fe(II)/Fe(III) ratio from Mössbauer spectroscopy (both the data presented in the main article (main) and here in the supporting information (SI)).

Sample	Crystal size $d_{XRD'}$(nm)	Lattice parameter (ang)	Fe(II)/Fe(III) (µXRD)	Fe(II)/Fe(III) (ferrozine)	Fe(II)/Fe(III) (Mössbauer, main)
Initial bio	10.04	8.4009	0.505	0.404 ± 0.005	0.45 ± 0.01
End ox 1 bio	9.68	8.3838	0.356	0.285 ± 0.014	0.39 ± 0.02
End red 1 bio	12.31	8.4038	0.532	0.754 ± 0.023	0.42 ± 0.01
End ox 2 bio	10.88	10.8841	0.152	0.297 ± 0.014	0.40 ± 0.02
End red 2 bio	17.47	17.4688	0.730	1.636 ± 0.095	0.42 ± 0.01
Initial abio	10.24	8.4038	0.532	0.434 ± 0.001	
End ox 1 abio	9.95	8.3891	0.399	0.436 ± 0.003	
End red 1 abio	9.97	8.4065	0.559	0.384 ± 0.006	
End ox 2 abio	10.24	10.2411	0.513	0.375 ± 0.028	
End red 2 abio	10.09	10.0865	0.448	0.410 ± 0.015	

Table S2. Fitting results of Mössbauer spectroscopy. δ – isomer shift; ΔE_Q – quadrupole splitting; B_{hf} – hyperfine magnetic field; stdev(B_{hf}) – standard deviation of hyperfine magnetic field; R.A. – Relative abundance; red. χ2 – goodness of fit.

Sample	Phase	δ (mm/s)	ΔE_Q (mm/s)	stdev(ΔE_Q) (mm/s)	B_{hf} (T)	stdev(B_{hf}) (T)	R.A. (%)	Error	Red. χ2
Start of ox. 1	Sextet 1	0.382	-0.016		49.6	0.1	37.2	1.4	1.19
	Sextet 2	0.674	-0.018		46.5	2.5	59.4	1.4	
	Doublet F(III)	0.477	0.709	6.5E-09			3.33	0.33	
End of ox. 1	Sextet 1	0.385	-0.023		49.7	0.4	42.3	2.6	0.86
	Sextet 2	0.626	-0.018		46.4	2.9	54.8	2.7	
	Doublet Fe(III)	0.341	0.564	4.5E-09			2.83	0.49	
End of red. 1	Sextet 1	0.379	-0.001		49.5	0.4	33.5	1.1	1.94
	Sextet 2	0.715	-0.043		46.4	2.6	48.6	1.1	
	Doublet Fe(II)	1.309	3.056	0.390			17.92	0.51	
End of ox. 2	Sextet 1	0.385	-0.041		49.7	0.8	33.8	2.0	1.06
	Sextet 2	0.629	-0.062		46.5	2.9	45.0	2.0	
	Doublet Fe(II)	1.309	3.105	0.369			9.87	0.70	
	Doublet Fe(III)	0.468	0.728	0.334			11.26	0.66	
End of red. 2	Sextet 1	0.364	0.0009		49.6	0.69	29.6	1.0	3.28
	Sextet 2	0.729	-0.076		46.6	3.0	43.5	1.1	
	Doublet Fe(II)	1.311	3.020	0.419			26.9	6.0	